JOURNAL OF MATERIALS SCIENCE 17 (1982) 691–700

Experimental studies of the fibre pull-out problem

E. BETZ
Department of Mechanical Engineering, The University of Newcastle, New South Wales, Australia

The fibre pull-out problem was studied experimentally using a method which enabled direct measurement of the energy release rate of de-bond and also observation of the fracture process involved. Preliminary test results indicated that the process was a two-stage one, with de-bond initiating at the fibre tip, followed later by de-bond initiating at the free surface end. If a flaw of sufficient size was present then a stage-two de-bond would occur. Results showed reasonable agreement between experimental results and computer measurements.

1. Introduction

This paper describes an experimental method designed to measure directly the energy release rate at fracture and also to observe the fracture process involved when an axisymmetric de-bond takes place between a fibre (represented by a glass rod) and the matrix in a fibre pull-out test. The method employed was similar to that used previously by Williams and Anderson [1], but recorded by photographic means the progress of crack propagation accurately and hence avoided the need of the finite element solution to completely analyse the results.

A preliminary test programme was carried out to check the performance of the equipment. The test results from this programme, which gave the energy release rate at fracture, compared favourably with those determined in a previous computer study of the fibre pull-out problem [1].

From these tests it was also shown that the fracture process in the absence of flaws, occurred in two stages, as illustrated in Fig. 1. The first stage began with a crack that initiated at the bottom surface of the embedded rod on axis "A" and propagated through adhesive fracture axisymmetrically across the bottom of rod to circular edge "B–B" in the diagram before continuing upward along the cylindrical surface of the rod for a short distance to "C–C", where the crack paused. The crack then changed direction moving outward into the matrix, forming an axisymmetric fracture cone through cohesive-fracture until propagation ceased at "D–D". After further pull-out displacement of the rod, a second-stage fracture process was initiated at a circular notch "E–E" formed by the rod and the free surface of the matrix. The crack extended downward uniformly along the cylindrical surface of the rod by adhesive fracture, passing through position "F–F", and finally linking up with the crack that was previously formed in the first stage process at "C–C" on the rod. When the flaw of sufficient length was inserted at either end, the stage-one fracture process was completely by-passed and the de-bond failure took place as a stage-two fracture process only.

A special flaw cutter was used for inserting a flaw at the free surface end to produce a stage-two de-bond process. Although a release agent was tried in order to insert a small flaw at the bottom end to induce a stage-one process and thus to measure the energy release rates, this method proved to be unsatisfactory. Hence, experimental results obtained from flaws at the free-surface end only could be used to compare the energy release rates measured and those obtained from the computer analysis.

A small aspect ratio was used in this work mainly for experimental convenience. However, the experiments showed that the main events of the fracture process occurred at the tip and the surface and the aim of the experiments to study

0022–2461/82/030691–10$03.70/0

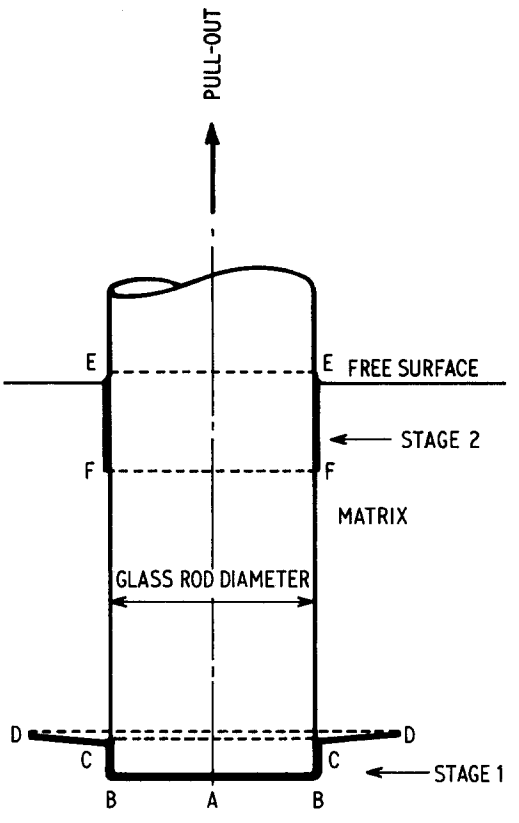

Figure 1 Two-stage fracture process (axisymmetric).

the initiation of the de-bonds would not be significantly affected by the small aspect ratio. The main events of the fracture process are particularly significant in the study of the failure modes in unidirectional fibre-reinforced composites where a fibre failure can be represented by the rod pull-out test, in which a redistribution of stresses to the adjacent fibres (as represented by the beaker in Fig. 2) is dependent on the fracture process during de-bonding of the broken fibre (as represented by the glass rod) [2].

2. Specimen preparation

The matrix for the specimen was cast from a fifty-fifty mixture by volume of Solithane® 113 urethane prepolymer and curing agent C113-300. This liquid mix was poured into 50 ml beaker to a depth of about 31 mm with the fibre (5 ± 0.05 mm diameter quartz glass rod) inserted axisymmetrically in the beaker at a gauge distance of 16.5 mm from the bottom, as shown in Fig. 2. The rods were held in position in the matrix during cure by a special jig (shown in Fig. 3) which could accommodate a batch of six specimens.

The specimens were placed in a vacuum chamber for de-gassing at room temperature for 8 h with the jig in a tilted position in the early stages of

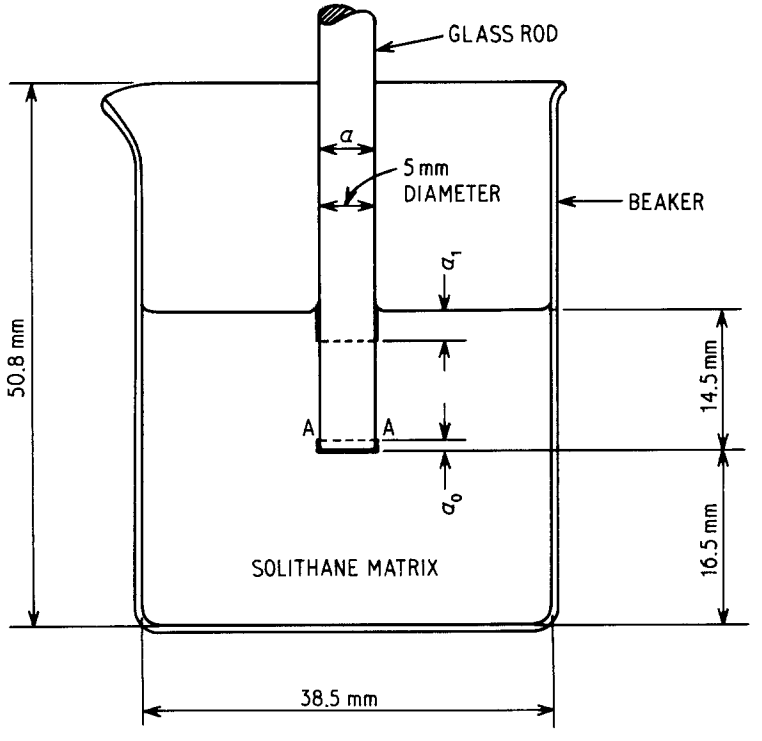

Figure 2 Dimensions of specimen in beaker.

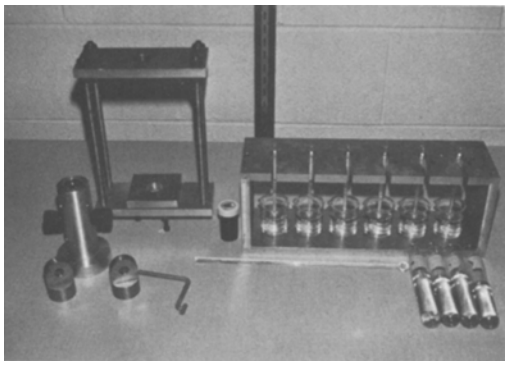

Figure 3 Jigs and moulds for casting and testing specimens.

de-gassing to remove bubbles that formed at the end of the rods. A slow cure of one week was used at room temperature to prevent thermal residual stresses of any significance from forming in the matrix. Attempts to produce flaws at the bottom end of the rod were made by precoating the required flaw area with Frekote® release agent. However, this coating did not produce a de-bond which would readily form a flaw, and the leading edge of the coating appeared to form a blunt crack, arresting crack growth. As mentioned in the introduction, this problem was solved at the surface end, where a specially designed cutter (Fig. 4) was employed to cut a flaw into the surface end, along the cylindrical surface "E–E–F–F" of the rod, as shown in Fig. 1.

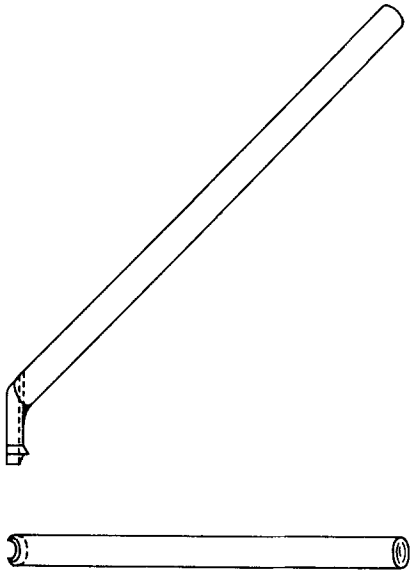

Figure 4 Flaw cutter.

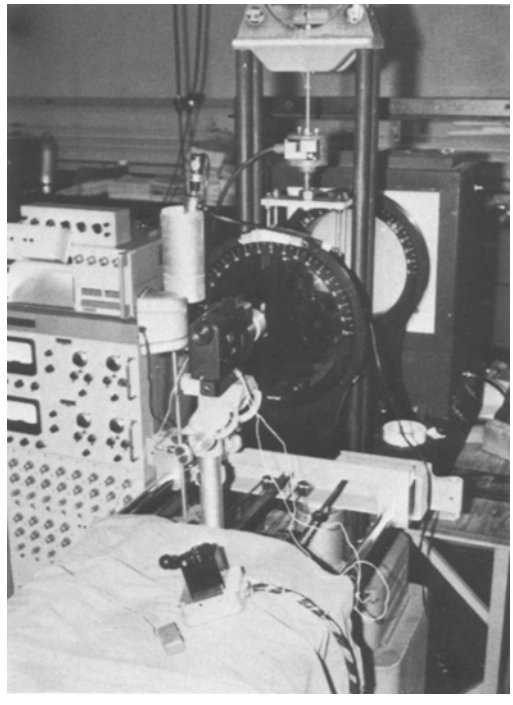

Figure 5 Test rig with visicorder at left, ciné camera in the centre and the polariscope and load frame in the background.

3. Test equipment

A small screw-type testing machine fitted with a load cell (type SR4) attached to the upper end of the testing machine frame was used to conduct the pull-out tests (see Fig. 5). The load-cell is shown attached to a loading cage fitted with a gimbal mounted load platform. The beaker containing the specimen was placed in an inverted position on the load platform, as shown in Fig. 6, with the free-

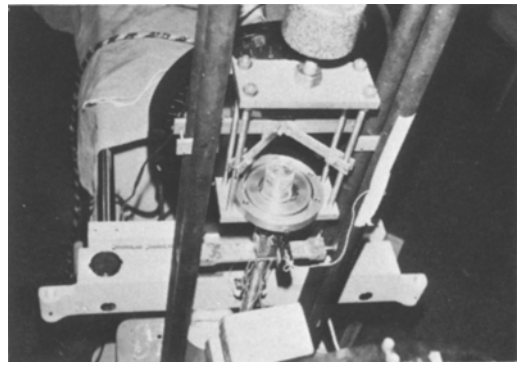

Figure 6 Gimbal mounted load platform with beaker containing specimen in inverted position. The clip gauge is shown in the front-centre (with wire attached) coupled to the glass rod protruding under the load platform.

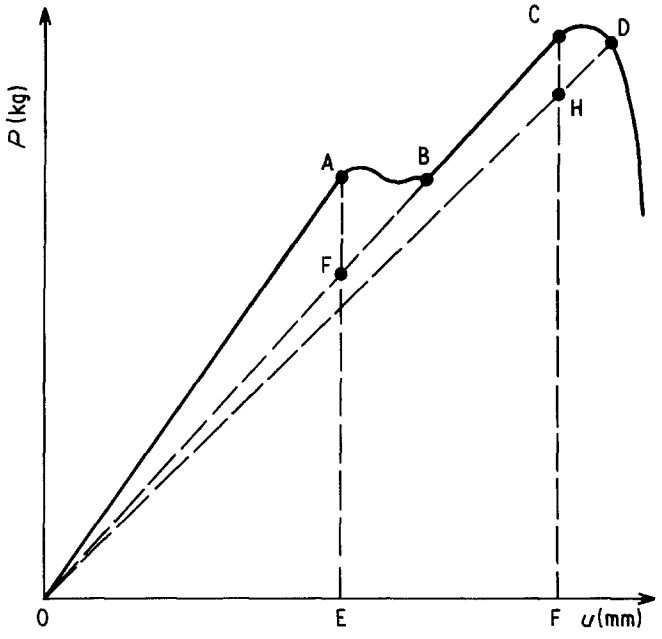

Figure 7 Force–displacement diagram for a two-stage fracture process.

surface end of the glass rod protruding through the load platform down to the cross-head of the testing machine. The glass rod was fitted with a ferrule to engage the jaw of the cross-head, and was prevented from slipping off by a bulb formed at the end of the glass rod. The gimbal mounting provided a means of self alignment for the specimen with the cross-head when placed axisymmetrically on the load platform. The symmetry of the specimen about the axis of the rod was important for the achievement of axisymmetric stress distributions within the matrix which is essential for a uniform crack-front advancement during a test. The cross-head was driven by gearing that was modified to give a constant cross-head speed of 0.98 mm per minute. A clip gauge, shown in the centre front of Fig. 6 with wire attached, measured the relative displacement between the rod and the beaker.

The force–displacment transducers were connected to the inputs of a Honeywell® signal

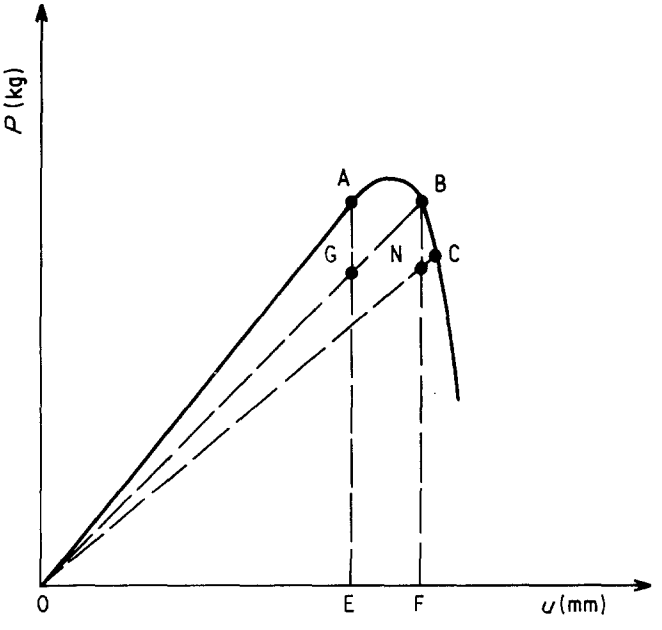

Figure 8 Force–displacement diagram for a stage-two fracture process only.

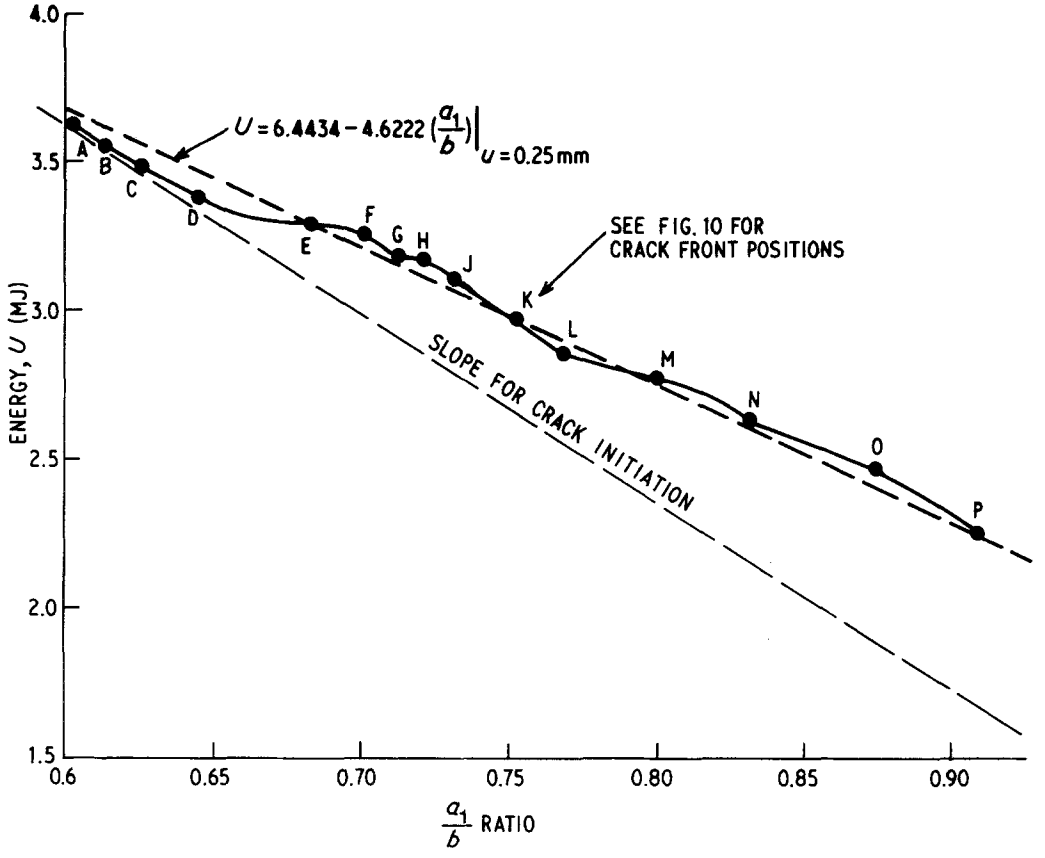

Figure 9 Energy, U, at displacement, normalized for $U = 0.25$ mm for Specimen 5.

conditioning unit with a visicorder unit attached (shown at left in Fig. 5). The visicorder is capable of recording both the force and displacement measurements on a constant-speed continuous chart, with time marking grids being superimposed by optical means during recording. A Nikon 8 mm ciné camera shown in the centre of Fig. 5, is fitted with suitable lens, and records on colour film, details of the crack growth and the surrounding isochromatic fringes that represent the three-dimensional stress distributions within the matrix. The polariscope used in the photoelastic studies is clearly seen in the background of Fig. 5. A digital time display was superimposed on each frame of the film to synchronize with the time markings made on the graphic records.

4. Analysis of test results

The test results obtained from the visicorder were plotted as force–displacement diagrams (see Figs 7 and 8). Then, for a given flaw size, a_0 (flaw size at the bottom or rod tip) or a_1 (flaw size at the free-surface end of the rod) (Fig. 2) the strain energy for crack extenion may be represented by the equation

$$G_A = \frac{\partial U}{\partial A}, \tag{1}$$

where G_A is the energy release rate at the critical conditions, that is, when the crack is on the verge of extending, U is the total potential energy and A is the surface area of the crack. In the case of an initial flaw at the bottom end of the rod, this condition corresponds to axisymmetric extension of Points A–A (Fig. 2) and the Point A on the force–displacement curve (Fig. 7). Whereas, if the initial flaw is at the free-surface end of the rod, the crack will extend axisymmetrically at points at a distance a_1 from the free-surface. This critical condition corresponds to Point A on the force–displacement curve (Fig. 8). However, the discussion will begin with experimental results obtained in the absence of an initial flaw.

Experiments showed that in the absence of an initial flaw (that is, both a_0 and a_1 are zero), de-bonding started at the bottom of the rod at the

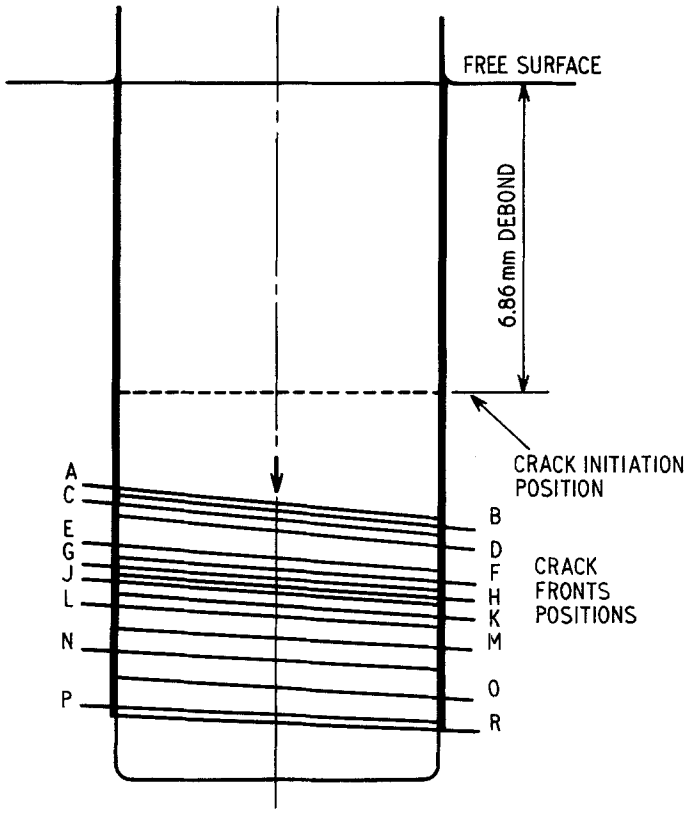

Figure 10 Crack growth for Specimen 5 (see Fig. 9).

loading axis, proceeded to the cylindrical edge, and then continued up the rod for a short distance before finally moving radially outward into the matrix to form an axisymmetric cone, whereafter further propagation ceased. This growth stage corresponds to part A–B of the load–displacement curve shown in Fig. 7. In the first stage of the fracture process the energy release rate (Equation 1) may be approximated by its average value over the part A–B (see Fig. 7).

$$G_{A-B} \simeq G_{A-B}|_{a_0=0} = \frac{S\,k}{\pi[(a^2/4) + a\delta a_0]}, \quad (2)$$

where S is the area OAFO, k is a scale factor, a is the diameter of the glass rod and $\pi a\,\delta a_0$ is the de-bonded area along the sides of the rod at the end of the first stage of the fracture process.

Continued displacement of the rod (along the part B–C of the curve in Fig. 7) ultimately initiated the second stage of fracture with de-bond at the free surface end of the rod. The crack propagated along the rod until complete de-bonding of the rod and matrix occurred. This stage corresponds to the part C–D of the load–displacement curve (Fig. 7). Again the energy release rate (Equation 1) may be approximated by its average value over the part C–D.

$$G_{C-D} \simeq \bar{G}_{C-D}|_{a_1=0} = \frac{S'k}{\pi a\delta a_1}, \quad (3)$$

where S′ is the area OCHO and $\pi a\delta a_1$ is the de-bonded area of the rod at the end of the second stage of fracture.

Up to now the fracture process had been considered in the absence of an initial flaw ($a_0 = a_1 = 0$). Let us now return to Equation 1, we examine the experimental evidence of a fracture process in the presence of an initial flaw a_0 (at the bottom of the rod) or a_1 (at the free surface of the rod).

As far as the initial flaw, a_0, is concerned the de-bonding followed the first two stages mentioned above except that in the first stage the de-bonding started at the tips of the initial flaw (points A–A in Fig. 2). If the initial flaw length, a_0, was sufficiently large, the first stage of the fracture process was completely absent. In general, however, in the first stage of the fracture process, the energy release rate (Equation 1) can be approximated as follows (see Fig. 7)

TABLE I Experimental results for different de-bonding situations

Specimen number	$\frac{a_0}{b}$ a_0 (mm)	U_{crit} (mm)	$\overline{G}$ (MJ/cm^{-2})	Remarks
1	$a_0 = 0$	1.1	19.4	Crack growth from rod bottom (Stage 1, Equation 2)
	$a_1 = 0$	1.4	8.3	Crack growth began from free-surface end (Stage 2, Equation 3)
2	$\frac{a_0}{b} = 0.14$ $a_0 = 0.20$	0.5	3.6	Crack growth from rod bottom release agent forming flaw (Stage 1, Equation 4)
	$a_1 = 0$	0.9	7.6	Non-uniform crack growth from free-surface end (Stage 2, Equation 3)
3	$\frac{a_0}{b} = 0$	0.7	13.4	Crack growth from rod bottom (Stage 1, Equation 2)
	$\frac{a_1}{b} = 0.10$ $a_1 = 0.14$	0.8	5.8	Crack growth from free-surface end (Stage 2, Equation 5)
4	$\frac{a_1}{b} = 0.15$ $a_1 = 0.19$	0.6	3.12	Stage 1 absent, crack growth from flaw cut into free-surface bond (Stage 2, Equation 6)
	$\frac{a_1}{b} = 0.17$ $a_1 = 0.20$	0.5	3.2	As above
	$\frac{a_1}{b} = 0.30$ $a_1 = 0.40$	0.5	3.8	As above

$$G_{A-B} \simeq \overline{G}_{A-B}|_{a_0} \equiv \left.\frac{\delta U}{\delta A}\right|_{a_0 \to a_0 + \delta a_0} = \frac{Sk}{\pi a a_0}. \quad (4)$$

The second stage of the fracture process follows exactly Equation 3 obtained previously.

In the presence of an initial flaw, a_1, at the free-surface end of the rod, two fracture mechanisms were possible. If the flaw surface length was sufficiently small it was observed that de-bonding took place in two stages identical to those discussed above. The first stage is represented by the energy release rate given by Equation 2 while in the second stage the energy Equation 1 may be represented by (Fig. 7)

$$G_{C-D} \simeq \overline{G}_{C-D}|_{a_1} \equiv \left.\frac{\delta U}{\delta A}\right|_{a_1 \to a_1 + \delta a_1} = \frac{S'k}{\pi a \delta a_1}. \quad (5)$$

However, when a flaw of sufficient length existed at the free-surface end of the rod, stage one of the fracture process was completely by-passed and the de-bonding took place as a stage-two failure only, as shown diagrammatically in Fig. 8. Experimental results for this type of failure are depicted in Figs 9 and 10. In this case the energy release rate (Equation 1) may be approximated as follows (Fig. 8)

$$G_{B-C} \simeq \overline{G}_{B-C}|_{a} \equiv \left.\frac{\delta U}{\delta A}\right|_{a_1 \to a_1 + \delta a_1} = \frac{S''k}{\pi a \delta a_1}, \quad (6)$$

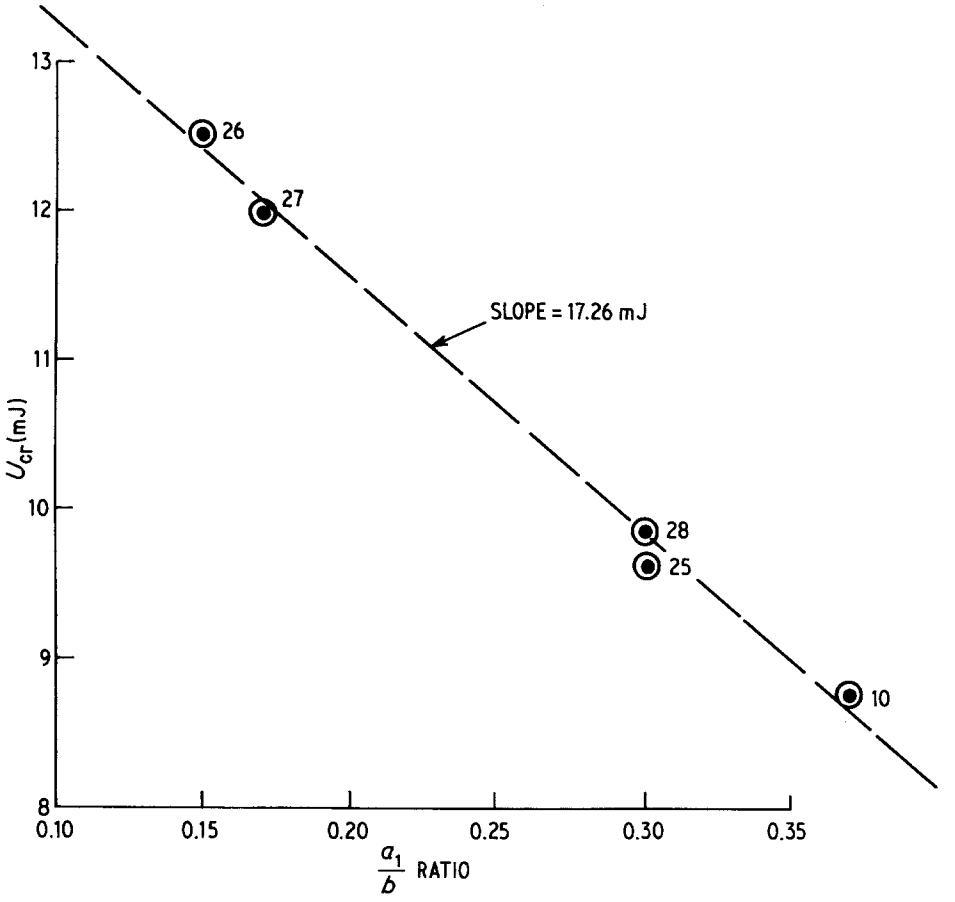

Figure 11 Energy, U, at critical conditions for five specimens (from [3]).

where

$$a_1 = a_1|_C - a_1|_B \tag{7}$$

and S″ is the area OBNO.

Typical experimental results for different de-bonding situations considered are summarized in Table I. The various stages of the fracture process observed in the individual situations are also indicated.

5. Discussion of results

In all approximate representations of the energy release rate (Equations 2 to 6) the approximate values are closer to the true value as $\delta a_x \to 0$. In practice, however, an error analysis would show that this may not be the case due to other measuring limitations. This seems to be borne out by the variations of $\overline{G}$ as obtained from U against a_1/b plots (see Fig. 9). It is seen that the average value

$$\overline{G}_{B-C}|_{U=0.25\,mm}$$

used in Equation 6 differs somewhat from the average value taken over the whole de-bonding process. This might conceivably be explained by, among other factors, uneven crack-front propagation and dynamic effects.

The one-specimen advancing-crack-front technique described above depends on the crack moving slowly with an even crack-front. Another technique, designed to overcome this disadvantage, is to determine the energy release rate in a number of identical specimens but with flaw sizes of different lengths. This technique was applied to five identical specimens with different flaw lengths (the flaws were introduced at the free-surface end

TABLE II Energy release rates

Specimen number	$\frac{a_1}{b}$	$\overline{G}_{experimental}$ (corrected for U)	$\overline{G}_{computer}$
4	0.15	31	20
	0.17	29	21
	0.3	31	29

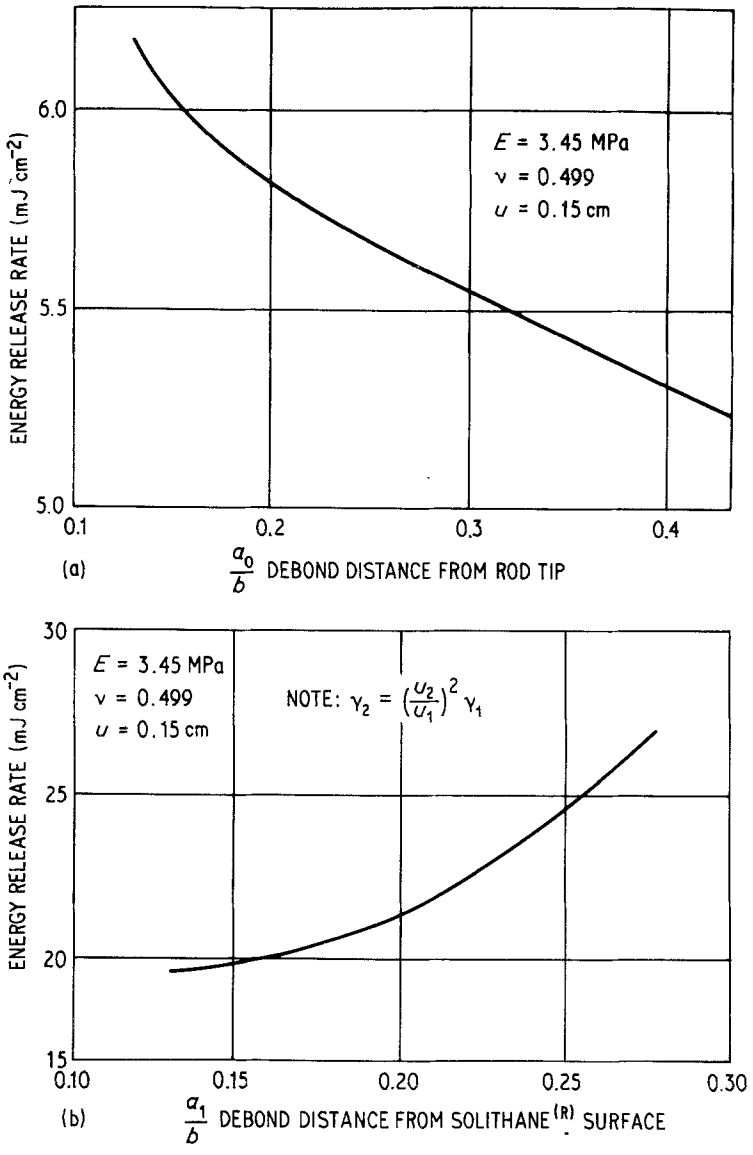

Figure 12 Computer results. (a) Energy release rate for rod-tip initial de-bond (after [1]). (b) Energy release rate for de-bond from Solithane® surface (after [1]).

of the rod, and were of such a length as to preclude stage one of the fracture). These results are plotted in Fig. 11 (and listed as Specimen 4 in Table I).

The energy release rates so obtained were adjusted according to the following equation (assuming linear elasticity for the matrix [1, 3, 4]),

$$\overline{G}_{\text{adjusted}} = \overline{G}_{\text{experimental}} \left(\frac{1.5}{U_{\text{critical}}} \right)^2 \quad (8)$$

and are compared in Table II with the appropriate computer values taken from Fig. 12. It is evident that the results are in reasonable agreement.

6. Conclusions

Test procedures have been developed, based on previous work of Williams and Anderson [1], to measure directly the adhesive fracture energy of de-bond. The innovation of photographing on ciné film the crack growth provided a very satisfactory method for measuring crack extension that could be accurately correlated with the appropriate forces, deflection and energy parameters. The photographic method provided a means to study the shape of the crack-front and the distribution of the stress in the matrix surrounding the rod. The gimbal mounting of the load platform in the load cage greatly assisted in the alignment of the specimen and helped to maintain an even axisymmetric crack-front growth and, hence, an axisymmetric stress distribution about the rod.

Preliminary test results were analysed and showed the fracture process for the specimens

tested to be a two-stage one, commencing with the first-stage de-bond, initiating at the bottom-end centre, with de-bond moving radially outward with an axisymmetric crack-front at the end and then for a short distance up the rod before turning radially outward to form an axisymmetric cone in the matrix where crack growth ceased. After further displacement of the rod the stage-two fracture initiated at the free-surface end and, under continued steady-rate displacement of the rod, the crack extended down the rod until the complete de-bond of the rod took place.

The energy release rate at critical conditions were measured by two techniques: the first technique described is referred to as the one-specimen advancing-crack-front technique; and the other technique used identical specimens but with various flaw lengths inserted. An attempt was made to produce flaws in the specimens with a release agent applied to prevent bonding of the rod to the matrix. This proved to be unsuccessful and a special flaw cutter was employed for use at the free-surface end only. It was observed that, if the flaw was of sufficient length, the stage-one fracture process was completely by-passed and de-bond failure occurred by a stage-two fracture process only. Results from the preliminary test programme for the stage-two fracture process were in reasonable agreement with computer results. The next stage of the investigations into the fibre pull-out problem involves a programme of testing for various diameter-to-length ratios in specimen geometry, coupled with further computer and a mathematical anslysis of the problem.

Acknowledgements

This programme was carried out by the author whilst on study leave at the University of Pittsburgh in 1979. The author wishes to thank Professor Max. L. Williams, Dean, Faculty of Engineering, University of Pittsburgh, for his help and encouragement in this study programme. I would also like to acknowledge the help of Associate Professor B. Karihaloo in the presentation of this work. This work was supported by Science Fracture Contract No. F 496 20 78 C 0101, Air Force Office of Scientific Research, U.S.A.

References

1. M. L. WILLIAMS and G. P. ANDERSON, Proceedings of the 4th Internation Conference on Fracture, Waterloo, Canada, June 1977 Vol 1, (Pergamon Press, New York, 1977).
2. P. W. BARRY, *J. Mater. Sci.* **13** (1978) 2177.
3. E. BETZ, University of Pittsburgh, Publication Number SETEC ME79-34 June, 1979.
4. J. A. BEGLEY and J. D. LANDES, Proceedings of the 1971 National Symposium on Fracture Mechanics, Part 2, Publication number STP 514 (American Society for Testing of Metals, Philadelphia, 1972).

Received 16 December 1980
and accepted 15 July 1981